Dynamic Evolution Simulation of Ablation Zone in Water-Jet Assisted Laser Machining of Korean Pine (*Pinus koraiensis*)

Yan Wang,[a] Bo Yan,[a] Ting Jiang,[a,b,]* Yueqiang Yu,[a,]* Tingang Ma,[a] Shuaiqi Huang,[a] Ziming Zheng,[a] Hao Wang,[a] and Kexin Ren [a]

In order to solve the difficulties with the observation of the ablation zone and the many factors that affect the dynamic evolution process of the ablation zone, the structural morphology and dynamic evolution process of the ablation zone in the process of water-jet assisted laser machining Korean pine (*Pinus koraiensis*) were studied. Based on the DFLUX subprogram, a compound heat source model was established. Under the comprehensive consideration of heat conduction, heat convection, heat radiation, and thermal physical properties varying with temperature, the three-dimensional (3D) finite element model of the Korean pine was numerically simulated by water-jet assisted laser machining. Through numerical simulation analysis, the cross-sectional morphology of Korean pine kerf was found to be screw-shaped, and the experimental results were in good agreement with the simulation results. The dynamic evolution law of water-jet assisted laser machining of Korean pine was obtained. In addition, as the laser power increased and the cutting speed decreased, the morphology of the Korean pine kerf remained unchanged, but the structure size of the Korean pine kerf showed an increasing change.

DOI: 10.15376/biores.17.3.4673-4688

Keywords: Laser technology; Water-jet assisted laser machining; Korean pine; Temperature field; Ablation zone

*Contact information: a: College of Mechanical Science and Engineering, Northeast Petroleum University, 99 Xuefu Road, Daqing, 163318, China; b: Ningbo Runyes Medical Instrument Co., Ltd. Ningbo, 315300, China; *Corresponding authors: jiangting1112@163.com; yuyaoqiang.1228@163.com*

INTRODUCTION

As a natural, green, and renewable material, wood is widely used in construction, packaging, furniture, and flooring industries, among others (Fleming *et al*. 2003; Seo *et al*. 2011; Fukuta *et al*. 2016). The increasing demand for wood has led to excessive consumption of wood resources. Therefore, improving the utilization rate of wood resources has become the focus of scholars around the world.

Laser processing technology has been applied to the field of wood processing to improve the yield of wood and reduce the processing allowance (Leone *et al*. 2009; Martínez-Conde *et al*. 2017). In particular, laser machining can overcome the limitations of traditional tool geometry when machining irregular curved wood products. Because wood has a low ignition point, gasification of wood occurs in an instant when impinged by the radiation of high-temperature laser. However, lower laser energy density causes the wood to burn, leading to a large heat-affected zone and carbon residue of the wood surface, which seriously affects the surface quality of the wood products (Panzner *et al*. 1998; Li *et*

al. 2018). Therefore, the realization of fine processing of wood products by laser has become a major challenge faced by the development of China's wood products processing industry, and a new processing technology is urgently needed (Eltawahni *et al*. 2011).

Hernández-Castañeda *et al.* (2010) studied the influence of dry and wet wood on the surface quality of laser-cut wood and concluded that the surface quality of laser-cut wet wood is better. With the in-depth study, the compressed gas auxiliary system was introduced to assist the laser cutting of wood, and the wood surface quality under different cutting parameters was studied. It was concluded that laser power and cutting speed are the main factors that affect the width of the wood kerf (Hernández-Castañeda *et al*. 2011). Yang *et al.* (2018) proposed the water-jet assisted YAG laser processing of Korean pine, and the water-jet pushed away the residues on the cutting surface to improve the surface quality of the processing area. Subsequently, the mechanism of wood processing assisted by YAG laser with water-jet was studied and good processing results were achieved (Yang *et al*. 2019). However, other studies have found that wood has a better absorption rate of carbon dioxide (CO_2) laser wave, and the CO_2 laser is advantageous because of its low price (Jiang *et al*. 2020; Jiang *et al*. 2021). Although there are many kinds of wood, Korean pine stands out as a coniferous wood with a uniform texture, light and soft feeling, delicate structure, beautiful shape and color, resistance to deformation, and strong resistance to degradation (Yusoff *et al*. 2008; Beck *et al*. 2009; Kačík and Kubovský 2011; Kubovský and Kacík 2014; Kubovský *et al*. 2016). Korean pine is widely used in finished wood products. Therefore, water-jet assisted CO_2 laser cutting of Korean pine is the focus of this study.

Korean pine products with complex geometric shapes and good surface qualities are difficult to make by traditional processes, but they can be crafted using water-jet assisted laser processing technology in wood crafts and other finishing fields. However, in the process of water-jet assisted laser processing, wood begins to decompose under the action of the energy generated by the laser beam, and the decomposition ends as the laser beam moves far away. This process is very complex and easily involves a series of highly nonlinear problems such as materials, geometry, and boundary conditions. Using the traditional theoretical calculation method and empirical method needs a long cycle and consumes human and material resources, so it can be difficult to obtain accurate research results. Currently, the finite element analysis method is an effective research method for water-jet assisted laser processing. Although there have been many published numerical simulation studies on hybrid laser-waterjet machining silicon and ceramic (Chen *et al*. 2014; Tangwarodomnukun *et al*. 2014; Zhao and Shrotriya 2017; Feng *et al*. 2018), there has been a lack of numerical simulation studies on water-jet-assisted laser processing of wood. Therefore, based on the finite element simulation theory, this paper analyzed the water-jet assisted laser processing process, established a three-dimensional (3D) finite element analysis model of Korean pine, conducted a temperature field simulation analysis, and studied the temperature field distribution and change rule of water-jet assisted laser processing Korean pine. The process parameter effects on the ablation zone, temperature distribution, and variation of the water-jet assisted laser processing of Korean pine were investigated. This research provides a strong theoretical support for the water-jet assisted laser machining of wood.

EXPERIMENTAL

Water-jet Assisted Laser Processing

The test process of water-jet assisted CO_2 laser cutting of Korean pine was carried out using a water-jet assisted CO_2 laser device (Fig. 1a), as outlined by Jiang *et al*. (2020). The machining direction of water-jet and laser can be seen in Fig. 1b. The wavelength of the CO_2 laser was 10.6 μm, the rated power of the laser was 80 W, and the focal length of the lens was 63.5 mm. The laser cutting machine was obtained from Shenzhen Baomei Technology Co. (Jinan, China). The diameter of the adjustable angle nozzle was 0.5 mm, and the water pressure at the nozzle was up to 2 MPa. Korean pine wood (Haicheng Machining Factory, Harbin, China) was used as the cutting material in the experiment. The air-dry density of the wood was 0.435 g/cm^3, and the moisture content was 12.62%. Korean pine is widely used in furniture and wood products because of its uniform texture, good structure, corrosion resistance, and moisture resistance. Korean pine needs to be treated before water-jet assisted laser cutting. The Korean pine was processed by traditional sawing to obtain profiles with the same size and uniform thickness. The wood was cut to dimensions of 100 mm × 60 mm × 2 mm (length × width × thickness). Before the Korean pine cutting test, 240 mesh sandpaper was used to polish the sample to improve its flatness.

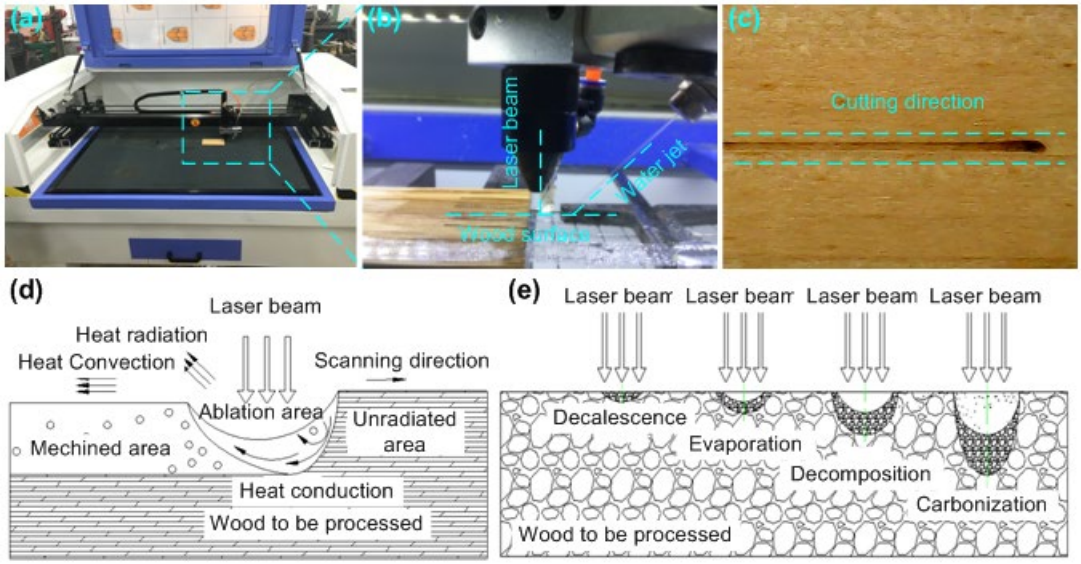

Fig. 1. The ablation process of water-jet assisted CO_2 laser machining Korean pine. The a) water-jet assisted CO_2 laser device, b) machining direction of water-jet and laser beam c) Korean pine specimen and its cutting method, d) schematic diagram of the heat transfer process, and e) schematic diagram of the laser ablation area

Figure 1c shows the Korean pine specimen and its cutting methods. During water-jet assisted CO_2 laser machining, when the laser energy acts on wood to be processed, the basic particles in the wood collide with laser photons. During this process, the laser energy is converted into heat and is absorbed by the wood. The heat absorbed by the wood can be divided into two parts. Some of the heat is transferred to the surrounding environment in the form of heat radiation and air heat convection, while the remainder of the heat is transferred to the interior of the wood to be processed in the form of heat conduction. The heat transfer process is shown in Fig. 1d. In the water-jet assisted laser processing of wood,

as the laser radiation time increases, the laser ablation of wood to be processed can be roughly divided into four stages. Figure 1e illustrates the ablation process, which is endothermic. Part of the absorbed energy diffuses to the surrounding environment due to the convection and radiation of the wood to be processed. The remainder of the energy is transferred to the interior of the wood by the heat transfer of the wood, which constitutes the energy that the wood absorbs. During the water evaporation process, the processed wood absorbs energy from the laser radiation. This increases the temperature of the wood, increases the thermal movement of free water molecules in the wood, and the water in the wood begins to evaporate. However, the chemical composition of the wood hardly changes during this process. In the process of wood decomposition, as the absorption of energy of wood increases, the temperature of wood increases, the free water of wood evaporates completely and loses bound water, and the wood begins to thermally decompose. The chemical composition of wood also begins to change. In the process of wood carbonization, as the energy absorbed by wood increases and the temperature continues to rise, wood decomposes and carbonizes. Previous research has found that the wood laser ablation area is relatively complex (Yue *et al*. 2013; Yu *et al*. 2015).

Finite Element Simulation of Water-jet Assisted Laser Machining

Analysis of heat transfer characteristics

During the water-jet assisted laser machining, the laser heat source acts on the surface of wood continuously with the change of time, and the wood surface is considered to be an infinite plane relative to the laser heat source. Therefore, during the numerical simulation analysis of water-jet assisted laser machining, the thermal conductivity differential equation in the rectangular coordinate system can be obtained by the first law of thermodynamics, as seen in Eq. 1:

$$c\rho\frac{\partial T}{\partial t}=[\frac{\partial}{\partial x}(\lambda\frac{\partial T}{\partial x})+\frac{\partial}{\partial y}(\lambda\frac{\partial T}{\partial y})+\frac{\partial}{\partial z}(\lambda\frac{\partial T}{\partial z})]+q_v \quad (1)$$

By converting the rectangular coordinate system to a cylindrical coordinate system, Eqs. 2, 3, and 4 can be obtained,

$$x=r\,cos\,\theta \quad (2)$$

$$y=r\,sin\,\theta \quad (3)$$

$$z=z \quad (4)$$

Based on Eqs. 1, 2, 3, and 4, the thermal conductivity differential equation in cylindrical coordinate system can be obtained using Eq. 5,

$$\rho c\frac{\partial t}{\partial \tau}=q_v+\frac{1}{r}\frac{\partial}{\partial r}(\lambda r\frac{\partial t}{\partial r})+\frac{1}{r^2}\frac{\partial}{\partial \theta}(\lambda\frac{\partial t}{\partial \theta})+\frac{\partial}{\partial z}(\lambda\frac{\partial t}{\partial z}) \quad (5)$$

Due to the constant change of time in the process of water-jet assisted laser machining, the laser heat source continuously acts on the ablation area of wood surface. The wood surface is much larger than the laser beam radius, so the wood surface can be regarded as an infinitely large plane. Therefore, Eq. 5 can be used to form Eq. 6,

$$\frac{1}{\alpha}\frac{\partial T}{\partial t}=\left(\frac{\partial^2 T}{\partial r^2}+\frac{1}{r}\frac{\partial T}{\partial r}+\frac{1}{r^2}\frac{\partial^2 T}{\partial \theta^2}+\frac{\partial^2 T}{\partial z^2}\right)+\frac{\dot{Q}}{\lambda} \quad (6)$$

where α is the thermal diffusivity of wood (m^2/s), namely, $\alpha=\lambda/(\rho\cdot c)$, T is the ablation temperature (K), t is the action time (s), r, φ, and z are the parameters of the cylindrical

coordinate system (m), and Q is the heat generated in the wood per unit time and volume (J).

It is assumed that when the surface heat source model is adopted, the heat generated in the wood is Q equal to 0, and the thermal action in the wood is relatively uniform. The heat source on the wood surface is in the form of a Gaussian distribution, and the temperatures at different positions along the heat source radius are different. The temperatures at points equidistant from the heat source center are the same, and no heat transfer occurs between the points. Because $\partial T/\partial\theta = 0$, Eq. 7 can be simplified as,

$$\frac{\partial T(r,z,t)}{\partial t} = \frac{\lambda}{c\rho}\left(\frac{\partial^2 T(r,z,t)}{\partial r^2} + \frac{1}{r}\frac{\partial T(r,z,t)}{\partial r} + \frac{\partial^2 T(r,z,t)}{\partial z^2}\right) \quad (7)$$

In the simulation analysis of the temperature field of water-jet assisted laser machining, according to the superposition principle, the superposition morphology can be obtained when the different time and position of the wood surface ablation area are superposed.

Heat Source Model and Scanning Path

In the actual process of water-jet assisted laser cutting wood, the width-depth ratio of the wood kerf are large, and a screw-shaped kerf section morphology is obtained. However, when the Gaussian surface heat source model or Gaussian rotating heat source model is used to simulate the water-jet assisted laser cutting wood, the section morphology is not consistent with the experimental results. Therefore, through analyzing the characteristics of different models, a compound heat source model consisting of Gaussian surface heat source model and Gaussian rotating body heat source model is constructed to simulate and analyze the temperature field of water-jet-assisted laser cutting wood. The schematic diagram of the compound heat source model is shown in Fig. 2(a), and the laser beam trajectory is shown in Fig. 2(b).

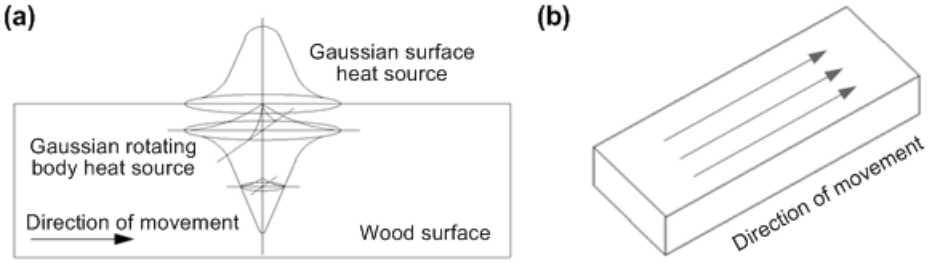

Fig. 2. The compound heat source model and laser beam path. (a) compound heat source model (b) laser beam trajectory

The thermal action of laser energy on wood surface is described by the Gaussian surface heat source model. The heat flux function can be seen in Eq. 8,

$$q(x,y,t) = \frac{\alpha\eta f_1 Q}{\pi\omega^2} exp(-2\frac{(x-x_0)^2+(y-y_0-v_0t)^2}{\omega^2}) \quad (8)$$

where $q(x, y, t)$ is the surface heat flux density (W/m^2); η is the absorption rate of wood; α is energy concentration coefficient; Q is the laser power (W); ω is spot radius (m); v_0 is the laser moving speed (m/s); and (x_0, y_0) is the starting point of the laser.

The thermal action of laser energy in wood is described by the Gaussian rotating

body heat source model, as shown in Eq. 9,

$$q(x,y,t) = \frac{6Q\eta f_2(H-\beta h)}{\pi R^2(2-\beta)} exp\left[\frac{-3[(x-x_0)^2+(y-v_0t)^2]}{R^2}\right] \quad (9)$$

where, $q(x, y, t)$ is the volume heat flux density (W/m^3); Q is the laser power (W); η is the absorption rate of wood; v_0 is the heat source cutting speed (m/s); t is the heat source action time (s); β is the attenuation coefficient; R is the effective action radius of body heat source (m); h is the arbitrary section height of heat source (m); and H is the effective action depth of body heat source (m).

The f_1 and f_2 variables in Eqs. 8 and 9 are the proportional coefficients of the total energy of the Gaussian surface heat source model and the Gaussian rotating body heat source model, that is, $f_1 + f_2 = 1$. The shape parameters ω, R, H, f_1, and f_2 of the compound heat source model can be obtained according to the test results and experimental experience.

Finite Element Model and Boundary Conditions

Finite element model

In the process of water-jet assisted laser machining, wood absorbs different energy in the X, Y, and Z directions due to the action of the laser heat source. The ablation region cannot be described by a two-dimensional model. Therefore, it is necessary to establish a 3D finite element geometric model and simplify it according to the actual process of water-jet assisted laser processing. The processed model can ensure the calculation accuracy and improve the calculation efficiency. Due to the small spot diameter of laser beam in the process of water-jet assisted laser machining, finite element model meshing is a very difficult problem in the process of temperature field simulation analysis, and the large number of meshing will reduce the calculation efficiency. Based on the above comprehensive consideration of accuracy and efficiency, the wood model is simplified in this paper. The size of the model is 3.0 mm × 1.2 mm × 0.5 mm, as shown in Fig. 3a. To ensure the normal simulation analysis of temperature field, several assumptions were made for the analysis model. Since the difference of thermal conductivity of wood along grain cutting and transverse grain cutting has little influence on the simulation results, wood can be regarded as isotropic and a continuous uniform medium, so heat transfer in all directions is the same. In the process of water-jet assisted laser machining, the radiation and convection coefficients between the wood surface and its surrounding medium are regarded as fixed values, which do not change with the change of temperature. The water-jet pressure is small with a minimal effect on wood cutting, so the impact of the water-jet in water-jet assisted laser machining can be ignored. The vaporization of wood ablation area in water-jet assisted laser machining is not considered.

Due to the large structure of the finite element geometric model selected in the simulation analysis of the temperature field of water-jet assisted laser machining, the local refinement method of the mesh is usually used in the mesh division of the finite element geometric model. This improves the solving efficiency without affecting the accuracy of the result. Therefore, the eight-node linear hexahedron element should be selected in this paper to mesh the geometric model of wood. The mesh of the action area of laser heat source was 0.05 mm, while the mesh of other areas was larger than 0.05 mm. The finite element mesh model of wood after segmentation is shown in Fig. 3b.

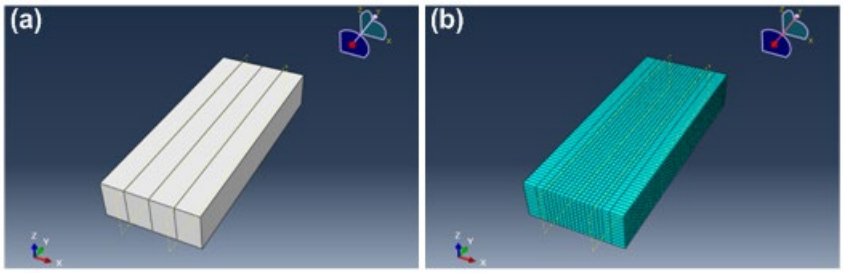

Fig. 3. The a) 3D finite element geometric model of wood and b) finite element mesh model of wood

Material properties of model

In the process of temperature field simulation analysis, the instantaneous high temperature generated by the laser will decompose and even burn the wood. The wood thermal property parameters will have highly nonlinear changes, so the specific heat capacity and thermal conductivity of wood are extremely important. In this paper, Korean pine was selected as the material for the temperature field simulation analysis. The specific heat capacity and thermal conductivity of Korean pine can be measured according to the national standard thermal physical parameters experiment. Table 1 shows the parameters such as specific heat capacity and thermal conductivity that change at different temperatures.

Table 1. The Thermal Properties of Korean Pine

Temperature (°C)	20	60	100	140	180
Coefficient of Thermal Conductivity (W/m·°C)	0.192	0.202	0.212	0.215	0.219
Specific Heat (J/kg·°C)	1,624	1,767	1,936	2,056	3,368
Density (kg/m^3)	435	435	435	435	435

As shown in Table 1, the thermal conductivity and specific heat capacity of Korean pine change nonlinearly with temperature, so the temperature field in the water-jet assisted laser processing of Korean pine is transient. In the temperature field simulation, the decomposition temperature of the Korean pine was 324.3 °C, the absorption rate of CO_2 laser beam was 0.95, the absorption rate of water was 0.865, and the laser spot diameter was 0.5 mm. The above data could be set through the property module and subprogram of Abaqus software (Dassault Systems, Vélizy-Villacoublay, France).

Initial and boundary conditions

In the temperature field simulation analysis of water-jet assisted laser machining wood, the ambient temperature of the wood at the beginning was taken as the initial condition of the model analysis. Therefore, when t is equal to 0, the wood is at room temperature, which yields Eq. 10,

$$T|_{t=0} = T_0 \quad (10)$$

The boundary conditions of the simulation analysis model were the interaction conditions between the wood surface and the surrounding medium. The boundary conditions of the simulation analysis model can be roughly divided into three categories, and its boundary load action is shown in Fig. 4.

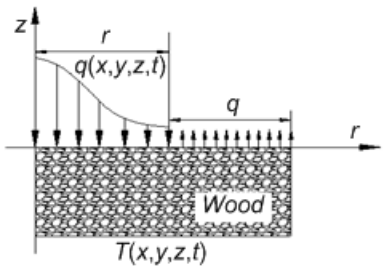

Fig. 4. The boundary load diagram of the temperature field simulation analysis

Given the temperature distribution function $T(x, y, z, T)$ of the wood boundary and the wood boundary area, the boundary condition I analyzed by the model can be seen in Eq. 11,

$$T|_{\Gamma} = T(x, y, z, t) \tag{11}$$

The temperature of the surface of the finite element model is the same as that of the medium around it, so the temperature function is usually constant (T_0=20 °C). The laser heat flux function $q(x, y, z, t)$ on the wood surface is known, which can be derived from the Fourier law. The boundary condition II derived by the Fourier law is described below in Eq. 12:

$$-\lambda(t)\frac{\partial T}{\partial n}|\Gamma = q(x, y, z, t) \tag{12}$$

The heat in the ablation area of the wood surface is usually the energy released by the laser beam emitted by the laser, which is loaded into the ablation area of wood surface in the form of heat flow density.

Radiation and convection will occur in the interaction between the wood surface and surrounding media, so boundary condition III can be described in Eq. 13,

$$-\mathrm{k}_e \frac{\partial T}{\partial z}\Big|_{z=0} + h(T_s - T_E) + \sigma\varepsilon(T^4 - T_E^4) = q \tag{13}$$

where T_s is the wood surface temperature (°C), T_E is the environment temperature (°C), h is the convective heat transfer coefficient (W/(m^2·°C)), ε is the coefficient of thermal radiation, and σ is the Stefan-Botzmann constant (approximately $5.67\times 10^{-8} W/(m^2 \cdot K^4)$).

In the process of water-jet assisted laser machining wood, the water-jet assisted laser processing equipment is open. Since the water droplets splashed by the water-jet will affect the laser processing, the water-jet does not directly spray to the wood surface. The wood is only in a water environment, so the wood and the water-jet have forced convection. Therefore, 0.8 is set as the effective radiation coefficient of wood, and 10,000 W/(m^2·°C) is the strong convection heat transfer coefficient between the wood and the water-jet.

Laser Heat Source Model Selection and Experimental Verification

Analysis of different heat source models

The heat decomposition temperature of Korean pine is 324.3 °C. Namely, the ablation temperature of laser cutting is equivalent to 324.3 °C. Therefore, the area with the higher surface temperature of Korean pine is the material ablation part, and the material in this part is decomposed and burned to form kerfs due to laser action. The area with the lower temperature is the non-ablation part, which is still solid after it is processed. The shape and size of the kerf can be obtained through the temperature field distribution of Korean pine in the simulation process of water-jet assisted laser machining. The structure morphology of the kerf is shown in Fig. 5. Part 5a of the figure shows that the depth to width ratio of the Korean pine kerf simulated by the Gaussian surface heat source model is relatively small, and the sectional morphology of the kerf formed by the Gaussian surface heat source model is flying-saucer shape. As shown in Fig. 5b, the depth-to-width ratio of the Korean pine kerf simulated by Gaussian rotating body heat source model is relatively large, and the sectional morphology is a deep hole. This paper adopted a compound heat source model to simulate the Korean pine kerf, which has a larger depth-to-width ratio and a screwed sectional morphology, as shown in Fig. 5c. The actual kerf morphology of the water-jet assisted laser machining Korean pine (along grain cutting) was observed using an FEI Quanta200 scanning electron microscope (Hillsboro, OR, USA), as shown in Fig. 5d. Therefore, compared with a single heat source, the compound heat source is closer to the actual status of water-jet assisted laser cutting Korean pine.

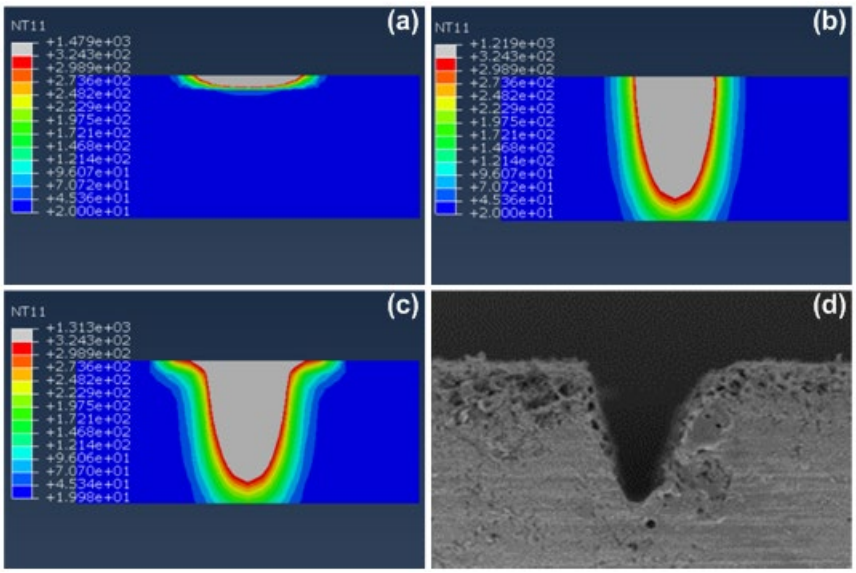

Fig. 5. The Korean pine kerf structure figures of water-jet assisted laser machining a) Gaussian surface heat source model, b) Gaussian rotational body heat source model, c) compound heat source model, and d) actual kerf morphology

Verification of heat source model test

Using the compound heat source model of water-jet assisted laser cutting Korean pine, a finite element simulation analysis according to water-jet assisted laser cutting Korean pine test results and experience is obtained. The test algorithm to obtain the size of the compound heat source model parameters, ω, R, H, as well as f_1 and f_2 (the proportion

coefficients Gaussian surface heat source and Gaussian rotating body heat source accounted for total power), and the related data are shown in Table 2.

Table 2. Process Parameters and Related Parameters of the Compound Heat Source Model

Sample Number	P (W)	V (mm/s)	ω (mm)	R (mm)	H (mm)	f_1 and f_2
1	10	30	0.25	0.17	0.38	0.65/0.35
2	12	30	0.25	0.18	0.4	0.6/0.4
3	14	30	0.26	0.19	0.4	0.6/0.4
4	16	30	0.28	0.18	0.41	0.65/0.35

When a defocusing amount of 2 mm, a flow pressure of 0.2 MPa, and a flow angle of 20º, the comparison results of the kerf morphology of the simulation analysis and experiment under different laser powers are shown in Fig. 6. As seen in Fig. 6, the kerf section morphology obtained by the simulation analysis is consistent with the cutting test, especially the transition region between the kerf and the surface.

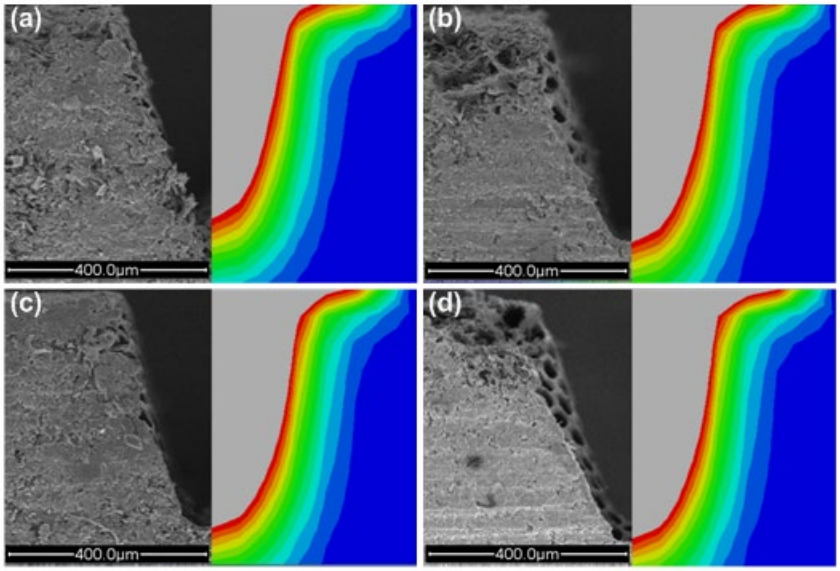

Fig. 6. The comparison between the experimental results and the simulation analysis results of water-jet assisted laser cutting Korean pine. a) P=10 W, b) P=12 W, c) P=14 W, and d) P=16 W

RESULTS AND DISCUSSION

Dynamic Evolution Law of Water-Jet Assisted Laser Cutting of Korean Pine

Figure 7 shows the temperature field changes in the ablation area of the Korean pine surface under different cutting times in the simulation process of water-jet-assisted laser machining when laser power is 12 W and cutting speed is 30 m/s. When the cutting time is 0 ms, the laser energy does not heat the ablation area of Korean pine surface, and the temperature of the ablation area of the Korean pine surface is equal to 20 °C at room temperature. When the cutting time is 0.04 ms, the laser energy heats the ablation area of Korean pine surface, and the temperature of ablation area increases over time. When the

cutting time is 0.2 ms, the temperature of the ablation area of the Korean pine rises as the laser energy action time increases. The heat diffuses to the surrounding area through heat transfer, convection, and radiation, among other ways. When the cutting time is 1 ms, the temperature of the ablation area of the Korean pine rises as the laser energy action time increases. The kerf boundary extends outward rapidly, and the kerf width and depth increase rapidly. When the cutting time is 5 ms, the temperature of the ablation area of the Korean pine rises as the laser energy action time increases. The kerf boundary continued to extend outward, albeit at a slower pace, and the kerf width and depth slowly increase. When the cutting time is 6 ms, the temperature of the ablation zone on the Korean pine surface rises as the laser energy action time increases, and the kerf boundary continues to extend outward at a very slow pace. The width and depth of the kerf are almost unchanged. At this time, the ablation temperature of the Korean pine surface almost reaches the maximum temperature, and the size of the Korean pine kerf reaches its maximum. In summary, the simulation process of water-jet assisted laser cutting of Korean pine is basically consistent with the actual cutting situation.

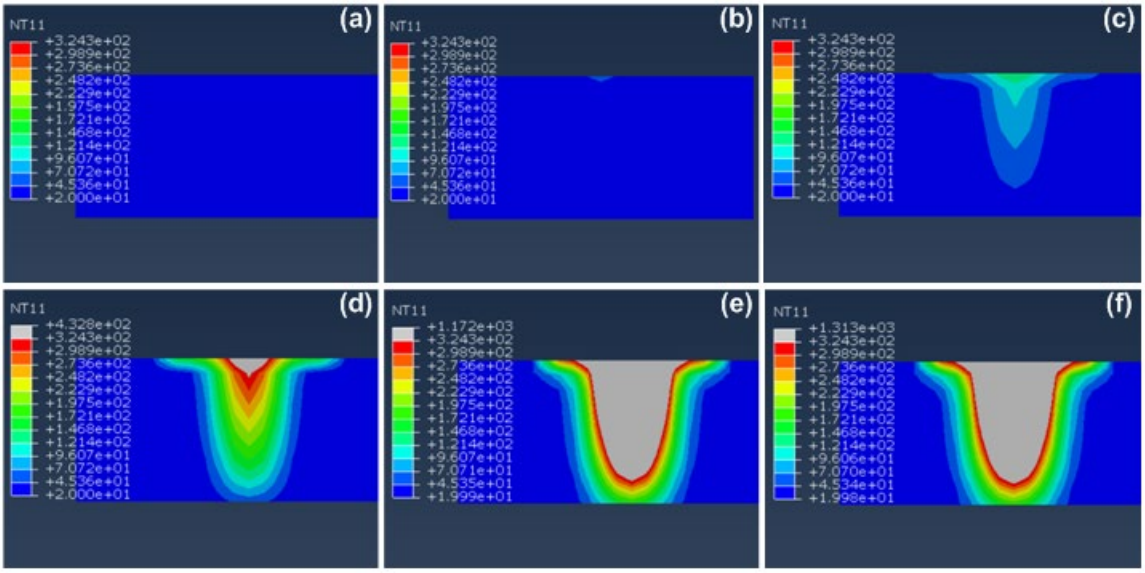

Fig. 7. Temperature field change cloud in the ablation area of water-jet assisted laser cutting of the Korean pine surface. a) *t*=0 ms, b) *t*=0.04 ms, c) *t*=0.2 ms, d) *t*=1 ms, e) *t*=5 ms, and f) *t*=6 ms

Influence of Laser Power on Temperature Field of Korean Pine Surface Ablation by Water-Jet Assisted Laser Machining

Figure 8 shows the kerf morphology and temperature field change curve of the Korean pine surface under different laser powers (10, 12, 14, 16, and 18W) when the cutting speed is 30 m/s. The model parameters in Fig. 9 were ω equal to 0.25 mm, R equal to 0.18 mm, H equal to 0.4 mm, f_1 equal to 0.6, and f_2 equal to 0.4. According to Figs. 8(a) to (e) the red dividing line is the decomposition line of Korean pine, and the internal temperature of the red dividing line exceeded the decomposition temperature of Korean pine. This formed the Korean pine kerf, namely the gray area. The structure size of the Korean pine kerf increases as the laser power increases, but the morphology of the Korean pine kerf does not change obviously. When the laser power increases from 10 to 12 W, the kerf depth and kerf width of the Korean pine increase little. When the laser power increases

from 12 to 16 W, there is a prominent increase in the kerf depth and kerf width of the Korean pine. When the laser power increases from 16 to 18 W, there is a small increase in the kerf depth and kerf width of the Korean pine. This is because when the laser power is small, Korean pine does not decompose quickly. As the laser power increases, the energy in the ablation area increases, the thermal decomposition of Korean pine speed is fast, and the Korean pine kerf structure size increases. However, when the laser power continues to increase, the thermal decomposition of Korean pine is slow, and the structure size of Korean pine kerf is reduced because the cooling effect of water flow and the coefficient of thermal conductivity of Korean pine are small. The effect of different laser powers on the temperature field distribution of the ablation region of Korean pine surface is basically the same. The laser power is closer to the kerf edge of Korean pine, the isotherm is denser, and the temperature shows uneven gradient diffusion from the kerf edge to the outside. Figure 8(f) shows the temperature field change curve in the whole analysis process. When the laser beam acts on the ablation area of the Korean pine surface, its temperature rises to the highest temperature quickly. When the laser beam is away from the ablation area of Korean pine surface, the temperature begins to decrease slowly. When the laser power increases from 10 to 18 W, the temperature change of the center of the Korean pine kerf is obvious and shows isometric change, where temperature value is approximately 207 °C.

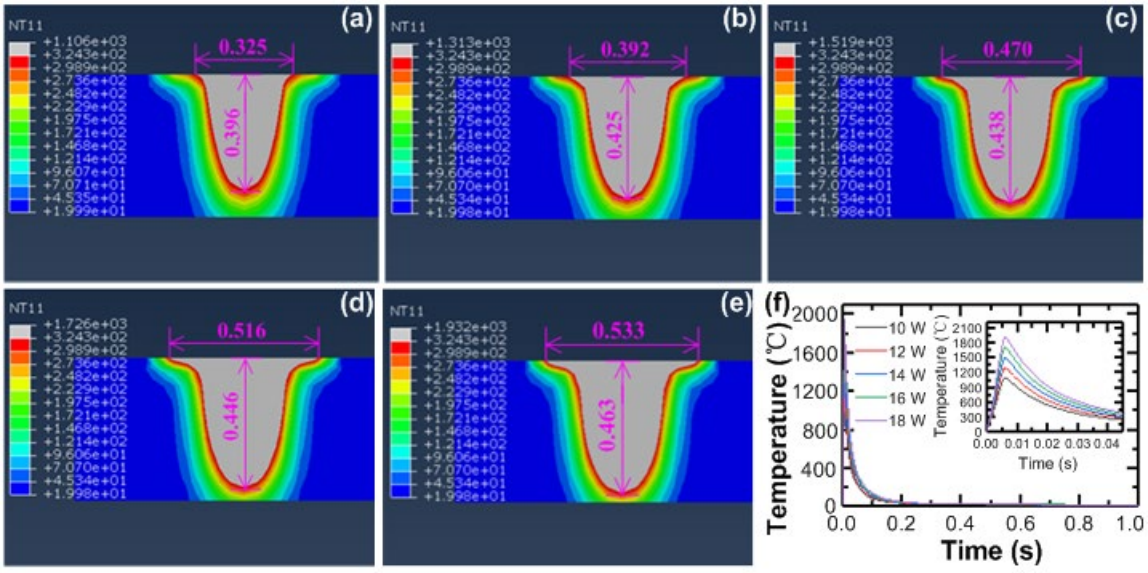

Fig. 8. Surface kerf morphology and temperature field change curves of the Korean pine under different laser powers. a) *P*=10 W, b) *P*=12 W, c) *P*=14 W, d) *P*=16 W, e) *P*=18 W, and f) the temperature change curves

Effect of Cutting Speed on Temperature Field of Korean Pine Surface Ablation by Water-Jet Assisted Laser

Figure 9 shows the kerf morphology and temperature field change curve of the Korean pine when the laser power is 12 W and the model parameters of the compound heat source model are as listed (ω=0.25 mm, R=0.18 mm, H=0.4 mm, f_1=0.6, and f_2=0.4) at different cutting speeds (20, 25, 30, 35, and 40 mm/s). According to Figs. 9(a) to (e), although the structure size of the Korean pine kerf decreases as the cutting speed increases,

the morphology of the Korean pine kerf does not change obviously. When the cutting speed increases from 20 to 30 mm/s, the depth and width of the Korean pine kerf decreases obviously. When the cutting speed increases from 30 to 35 mm/s, the depth and width of the Korean pine kerf decrease slightly. When the cutting speed increases from 35 mm/s to 40 mm/s, the depth and width of the Korean pine kerf decrease prominently. This is because when the cutting speed is small, the time of laser energy acting on the ablation area of the Korean pine surface increases. This causes the surface temperature of the Korean pine to reach the decomposition temperature quickly and promote the rapid decomposition of Korean pine, thereby increasing the structure size of the kerf. As the cutting speed increases, the time of laser heat source acting on the ablation area of Korean pine surface decreases, resulting in less heat absorption in the ablation area of the Korean pine surface, a slow thermal decomposition of Korean pine, and a reduced structure size of the Korean pine kerf. At different cutting speeds, the temperature field in the ablation area of the Korean pine surface is basically the same. The laser power is closer to the kerf edge of Korean pine, the isotherm is denser, and the temperature shows uneven gradient diffusion from the kerf edge to the outside. Figure 9(f) shows the temperature field change curve in the whole analysis process. When the laser beam acts on the Korean pine surface ablation area, its temperature rises to the highest temperature quickly. When the laser beam is away from the ablation area of the Korean pine surface, the temperature begins to decrease slowly. When the cutting speed increases from 20 to 40 mm/s, the temperature change of the center of the Korean pine kerf is obvious but it decreases gradually, where the maximum of the change in temperature is 277 °C and the minimum value is 121 °C.

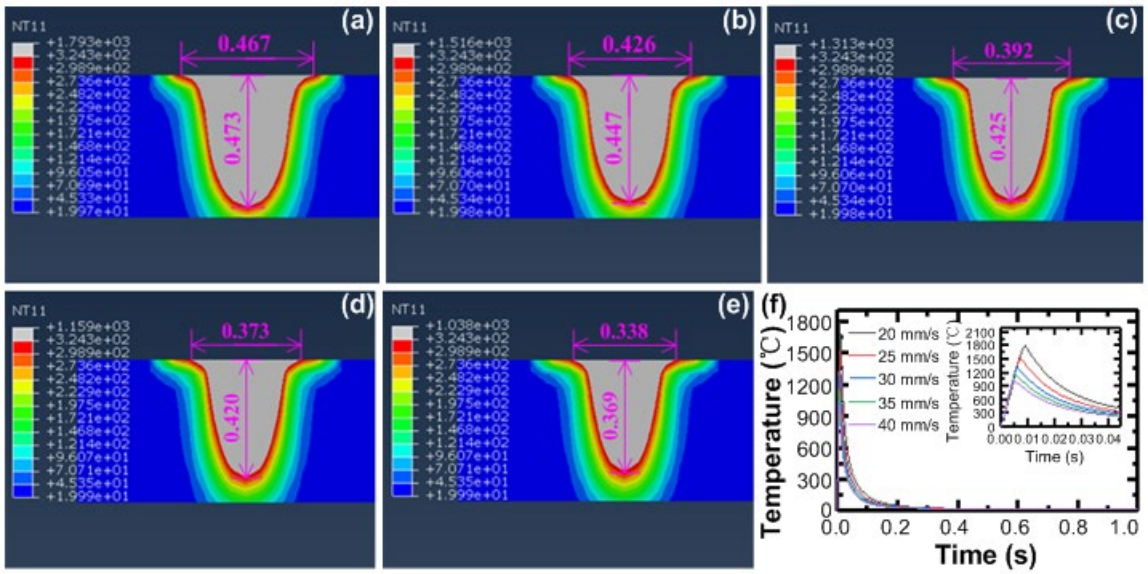

Fig. 9. The surface kerf morphology and temperature field change curves of the Korean pine at different cutting speeds. a) *V*=20 mm/s, b) *V*=25 mm/s, c) *V*=30 mm/s, d) *V*=35 mm/s, e) *V*=40 mm/s, and f) the temperature change curves

CONCLUSIONS

1. Based on the heat source model theory of finite element simulation analysis, a compound heat source model was established in line with the simulation analysis of water-jet-assisted laser cutting Korean pine. By programming the DFLUX subroutine file, the heat flux load and cutting trajectory control were realized. According to the actual processing situation of water-jet assisted laser machining, the model was analyzed and simplified, and the 3D finite element model of water-jet assisted laser cutting Korean pine was established and meshed, which could improve the accuracy of simulation results and the calculation efficiency.
2. Through the simulation analysis of water-jet assisted laser cutting Korean pine, the sectional morphology of the kerf formed by the Gaussian rotating body heat source model was deep hole. The sectional morphology of the kerf formed by the Gaussian rotating body heat source model also was deep hole. The sectional morphology was screw using a compound heat source model. By comparison, the sectional morphology of the Korean pine kerf using a compound heat source model was more consistent with the actual situation of the water-jet assisted laser cutting Korean pine.
3. The temperature field of the water-jet assisted laser cutting Korean pine was analyzed with the compound heat source model. The dynamic evolution law of water-jet assisted laser machining Korean pine was obtained. In addition, as the laser power increased and the cutting speed decreased, the morphology of the Korean pine kerf remained unchanged, but the structure size of the Korean pine kerf increased.

ACKNOWLEDGMENTS

The authors are grateful for the support of the Northeast Petroleum University Guiding Innovation Fund Project (2021YDL-13) and the Northeast Petroleum University Scientific Research Start-up Fund projects (2019KQ67 and 2021KQ09).

REFERENCES CITED

Beck, K., Salenikovich, A., Cloutier, A., and Beauregard, R. (2009). "Development of a new engineered wood product for structural applications made from trembling aspen and paper birch," *Forest Products Journal* 59(7/8), 31-35.

Chen, C., Yuan, G., and Wang, J. (2014). "Low-pressure water-jet and laser composite cutting on Al_2O_3 ceramic," *Infrared and Laser Engineering* 7, 2097-2102.

Eltawahni, H. A., Olabi, A. G., and Benyounis, K. Y. (2011). "Investigating the CO_2 laser cutting parameters of MDF wood composite material," *Optics and Laser Technology* 43(3), 648-659. DOI: 10.1016/j.optlastec.2010.09.006

Feng, S., Huang, C., Wang, J., and Zhu, H. (2018). "Material removal of single crystal 4H-SiC wafers in hybrid laser-waterjet micromachining process," *Materials Science in Semiconductor Processing* 82, 112-125. DOI: 10.1016/j.mssp.2018.03.035

Fleming, M. R., Hoover, K., Janowiak, J. J., Fang, Y., Wang, X., and Liu, W. (2003). "Microwave irradiation of wood packing material to destroy the Asian longhorned

beetle," *Forest Products Journal* 53(1), 46-52.

Fukuta, S., Ogawa, K., Nomura, M., Yamasaki, M., and Sasaki, Y. (2016). "Sound insulation of walls using wood insulation mat and plywood jointed with a combination of adhesive tape and wood dowels," *European Journal of Wood and Wood Products* 75(4), 595-602. DOI: 10.1007/s00107-016-1085-3

Hernández-Castañeda, J. C., Sezer, H. K., and Li, L. (2010). "Dual gas jet-assisted fibre laser blind cutting of dry pine wood by statistical modelling," *The International Journal of Advanced Manufacturing Technology* 50(1-4), 195-206. DOI: 10.1007/s00170-009-2491-z

Hernández-Castañeda, J. C., Sezer, H. K., and Li, L. (2011). "The effect of moisture content in fibre laser cutting of pine wood," *Optics and Lasers in Engineering* 49(9-10), 1139-1152. DOI: 10.1016/j.optlaseng.2011.05.008

Jiang, T., Yang, C., Yu, Y., Doumbia, B. S., Liu, J., and Ma, Y. (2021). "Prediction and analysis of surface quality of northeast China ash wood during water-jet assisted CO_2 laser cutting," *Journal of Renewable Materials* 9(1), 119-128. DOI: 10.32604/jrm.2021.011490

Jiang, T., Yang, C., Yu, Y., Lou, Y., Liu, J., and Ma, Y. (2020). "Water-jet assisted laser cutting of Korean pine (*Pinus koraiensis*): Process and parameters optimization," *BioResources* 15(2), 2540-2549. DOI: 10.15376/biores.15.2.2540-2549

Kačík, F., and Kubovský, I. (2011). "Chemical changes of beech wood due to CO_2 laser irradiation," *Journal of Photochemistry and Photobiology A: Chemistry* 222(1), 105-110. DOI: 10.1016/j.jphotochem.2011.05.008

Kubovský, I., and Kacík, F. (2014). "Colour and chemical changes of the lime wood surface due to CO_2 laser thermal modification." *Applied Surface Science* 321, 261-267. DOI: 10.1016/j.apsusc.2014.09.124

Kubovský, I., Kacík, F., and Reinprecht, L. (2016). "The impact of UV radiation on the change of colour and composition of the surface of lime wood treated with a CO_2 laser," *Journal of Photochemistry and Photobiology A: Chemistry* 322-323, 60-66. DOI: 10.1016/j.jphotochem.2016.02.022

Leone, C., Lopresto, V., and De Iorio, I. (2009). "Wood engraving by Q-switched diode-pumped frequency-doubled Nd:YAG green laser," *Optics and Lasers in Engineering* 47(1), 161-168. DOI: 10.1016/j.optlaseng.2008.06.019

Li, R., Xu, W., Wang, X. A., and Wang, C. (2018). "Modeling and predicting of the color changes of wood surface during CO_2 laser modification," *Journal of Cleaner Production* 183, 818-823. DOI: 10.1016/j.jclepro.2018.02.194

Martínez-Conde, A., Krenke, T., Frybort, R., and Müller, U. (2017). "Review: Comparative analysis of CO_2 laser and conventional sawing for cutting of lumber and wood-based materials," *Wood Science and Technology* 51(4), 943-966. DOI: 10.1007/s00226-017-0914-9

Panzner, M., Wiedemann, G., Henneberg, K., Fischer, R., Wittke, T.-H., and Dietsch, R. (1998). "Experimental investigation of the laser ablation process on wood surfaces," *Applied Surface Science* 127-129, 787-792. DOI: 10.1016/s0169-4332(97)00743-5

Seo, J., Jeon, J., Lee, J.-H., and Kim, S. (2011). "Thermal performance analysis according to wood flooring structure for energy conservation in radiant floor heating systems," *Energy and Buildings* 43(8), 2039-2042. DOI: 10.1016/j.enbuild.2011.04.019

Tangwarodomnukun, V., Wang, J., Huang, C. Z., and Zhu, H. T. (2014). "Heating and

material removal process in hybrid laser-waterjet ablation of silicon substrates," *International Journal of Machine Tools and Manufacture* 79, 1-16. DOI: 10.1016/j.ijmachtools.2013.12.003

Yang, C., Jiang, T., Yu, Y., Dun, G., Ma, Y., and Liu, J. (2018). "Study on surface quality of wood processed by water-jet assisted nanosecond laser," *BioResources* 13(2), 3125-3134. DOI: 10.15376/biores.13.2.3125-3134

Yang, C., Jiang, T., Yu, Y., Bai, Y., Song M., Miao, Q., Ma, Y., and Liu, J. (2019). "Water-jet assisted nanosecond laser microcutting of northeast China ash wood: Experimental study," *BioResources* 14(1), 128-138. DOI: 10.15376/biores.14.1.128-138

Yu, M., Song, S., Jiang, S. H., Ma, Y., and Ren, H. E. (2015). "Theory research of wood surface cells explosion heated by nanosecond laser," *Forestry Machinery & Woodworking Equipment* 43(2), 30-32. DOI: 10.3969/j.issn.2095-2953.2015.02.012

Yue, W., Ando, K., and Hattori, N. (2013). "Changes in the anatomy of surface and liquid uptake of wood after laser incising," *Wood Science and Technology* 47(3), 447-455. DOI: 10.1007/s00226-012-0497-4

Yusoff, N., Ismail, S. R., Mamat, A., and Ahmad-Yazid, A. (2008). "Selected Malaysian wood CO_2-laser cutting parameters and cut quality," *American Journal of Applied Sciences* 5(8), 990-996. DOI: 10.3844/ajassp.2008.990.996

Zhao, J., and Shrotriya, P. (2017). "Increase the hardness of polycrystalline cubic/wurtzite boron nitride composite through hybrid laser/waterjet heat (LWH) treatment," *Advances in Applied Ceramics* 116(6), 333-340. DOI: 10.1080/17436753.2017.1320062

Article submitted: February 7, 2022; Peer review completed: May 21, 2022; Revised version received: June 17, 2022; Accepted: June 18, 2022; Published: June 21, 2022.
DOI: 10.15376/biores.17.3.4673-4688